Available online at www.sciencedirect.com
SCIENCE DIRECT
Carbon xxx (2006) xxx–xxx
CARBON
www.elsevier.com/locate/carbon

Tearing, folding and deformation of a carbon–carbon sp^2-bonded network

L.X. Li, R.P. Liu *, Z.W. Chen, Q. Wang, M.Z. Ma, Q. Jing, G. Li, Y. Tian

State Key Laboratory of Metastable Materials Science & Technology, Yanshan University, Qinhuangdao 066004, PR China

Received 23 October 2005; accepted 14 December 2005

Abstract

A monolayer and a few layers of carbon sp^2-bonded networks were torn and folded by the tip of an atomic force microscope at the steps on newly cleaved highly oriented pyrolytic graphite. It was found that the preferential breaking directions and folding axes are along the symmetry directions of the graphite hexagonal structure. Depending on the force exerted by the tip, breaking may occur along other directions. The torn part of the graphene sheet can even be stretched and deformed, and does not resume its original shape after release from the tip.

Keywords: Synthetic graphite; Surface treatment; Cracking; Atomic force microscopy; Mechanical properties

1. Introduction

The carbon–carbon sp^2 bond is one of the strongest chemical bonds [1,2]. Typical materials with such bonds include graphene sheets, carbon nanotubes (CNTs) and fullerenes. Among these, CNTs have received significant attention since their discovery [3] due to the measured and theoretically predicted impressive mechanical properties [4–8]. CNTs can be seen as graphene sheets wrapped into cylinders. Therefore CNTs have very similar mechanical properties as a graphene sheet. The major features of the structure of graphite are the hexagonal pattern that repeats itself periodically in-plane and the ABABA...stacking between planes [9]. As a result of the periodicity, each atom is bonded to three neighbouring atoms in-plane. Such a structure is mainly due to the sp^2 hybridization in which one s-orbital and two p-orbital electrons combine to form three hybrid sp^2-orbitals at 120° to each other within a plane. This covalent bond, referred to as the σ-bond, is a strong chemical bond and plays an important role in the impressive mechanical properties of CNTs. The out-of-plane bond, referred to as the π-bond, is relatively weak. One layer of graphite is showed in Fig. 1.

To understand the mechanical properties of sp^2-bonded network, preferential tearing and folding directions of a monolayer of graphite have been studied by atomic force microscope (AFM) and scanning tunnelling microscope [10–12], but without details on the tearing and folding directions when the tearing force is different from these directions.

2. Experimental

Highly oriented pyrolytic graphite was cleaved to form fresh surfaces. Observations with an AFM (NT-MDT P47) using the tapping mode show that there are some parallel steps on the fresh surface (Fig. 2a). In order to reveal the breaking, folding and deformation of the graphite layers, the rigid silicon tip of the AFM was used to tear the graphite layers by moving it against the steps. The torn surface was then observed by the AFM, as shown in Fig. 2b. Cross-sectional analysis shows that the thickness of the torn layers is one or two atomic layers.

* Corresponding author. Fax: +86 335 8074723.
E-mail address: riping@ysu.edu.cn (R.P. Liu).

0008-6223/$ - see front matter © 2006 Elsevier Ltd. All rights reserved.
doi:10.1016/j.carbon.2005.12.031

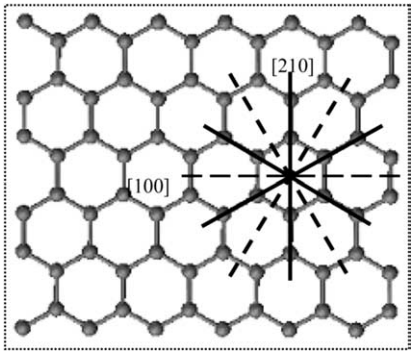

Fig. 1. Hexagonal network of a graphite monolayer with its symmetry axes indicated.

3. Results and discussion

Through observation, it was found that all of the folding axes are parallel to each other with the angle of 30° to the direction of the steps. And most of the breaking directions are parallel to each other too, but with the angle of 120° to the direction of the steps. In order to show more clearly the breaking and folding feature of the graphite layer, the torn part pointed by an arrow (Fig. 2b) is magnified with some special points, lines, angles and triangles named with letters (Fig. 2c). Line *abc* is the edge of the step, *b* the point where the tip touched the step firstly, line *be* the breaking direction (where the bonds were broken), line *ce* the folding axis, $\triangle dce$ the torn part and $\triangle bce$ the part folded around the *ce* axis. In this case, there are the following relations: $\triangle bec \cong \triangle dec$, $\angle abe = 120°$, $\angle bec = 90°$, and $\angle bce = \angle dce = 30°$.

Breaking and folding preferentially along the symmetry directions of graphite are in agreement with the previous results [10–12]. The reason why the breaking and folding preferentially occur along the symmetry directions stems from the carbon sp^2-bonded hexagonal network structure.

It is quite understandable that the breaking of the bond took place between two bonded atoms. Thus, there are three possibilities, l_h, m_h and n_h ($h = 1, 2, 3$), for breaking a single atomic layer (Fig. 3). Each possibility has three equivalent directions with 120° to each other. The easiest propagating direction of breaking, from the energetic point of view, is along the direction l_h, [1 0 0], which is the connection of the midpoints of the opposite sides of the hexagons of the graphene sheet. For breaking along this direction, the minimum energy is required [13] and no Stone–Wales bond rotation resulting in pentagon–heptagon–heptagon–pentagon (5–7–7–5) topological defect [14–16] is needed.

For analyzing the preferential folding axis, it is supposed that the axis around which the graphene sheet was folded go through two carbon atoms within each single hexagonal ring, otherwise the bond between the two atoms will be folded in space, which is impossible because the bond must be along a straight line between the two atoms. If it is further assumed that the hexagonal structure was not distorted, there are two possibilities for folding, around

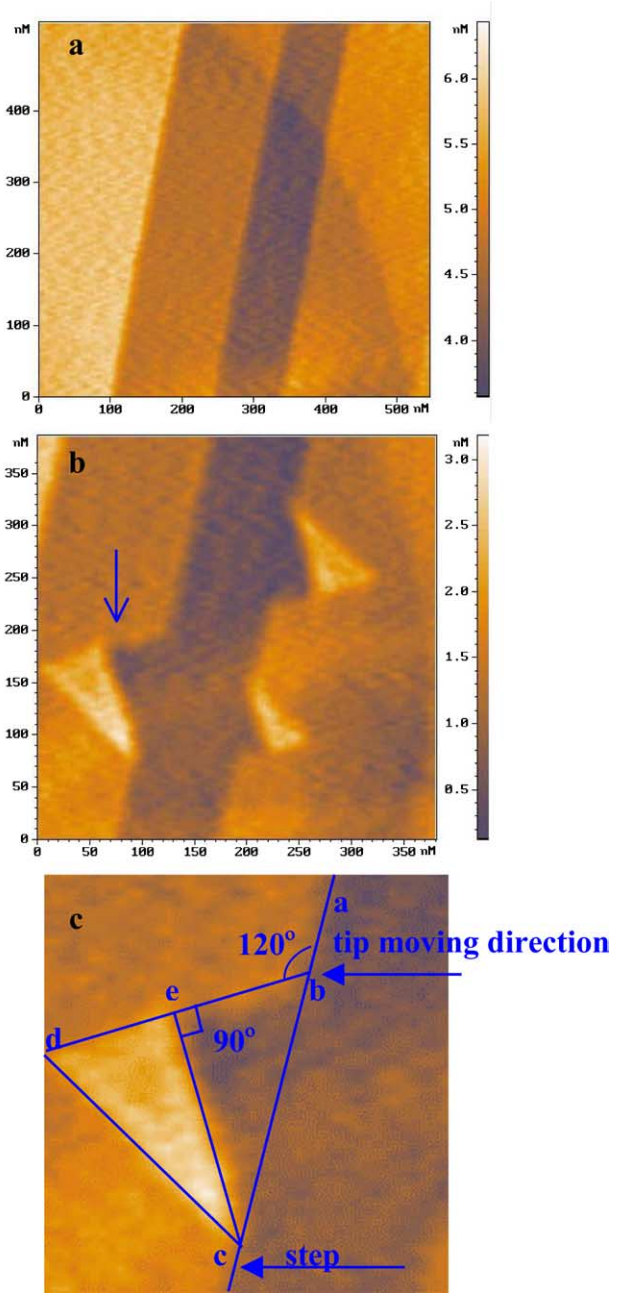

Fig. 2. AFM images of the surfaces of highly oriented pyrolytic graphite. (a) Newly cleaved surface with some parallel steps. (b) Surface with two atomic layers torn by an AFM tip at the steps. (c) Magnification of the part pointed by an arrow in (b), *abc* standing for the step edge, *b* the firstly torn point, *be* the breaking direction, *ce* the folding axis, triangle *dce* the graphite torn and folded.

axes *o–o* [2 1 0] and *p–p* [1 0 0]. Each possibility has three equivalent axes. From the energy calculation of the nanotubes wrapped around these two different axes, it is 0.38 eV/atom lower around *o–o* axis than around *p–p* axis. Folding around any other axes will cause the distortion of the network, which largely increases the energy. Therefore the most possible axis is *o–o* from the energetic point of view.

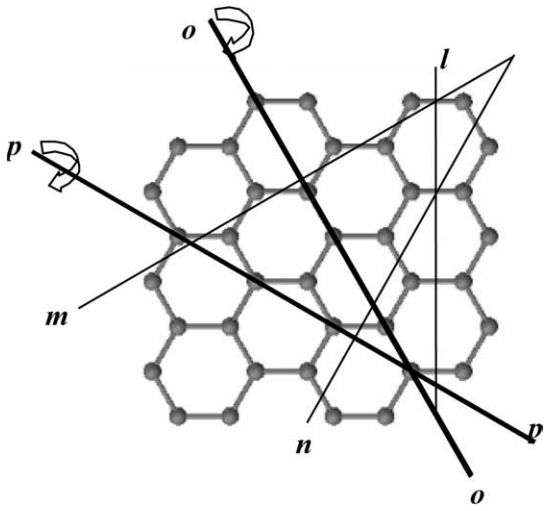

Fig. 3. Possible breaking directions and folding axes. *l*, *m* and *n* are three possible breaking directions; and *o*–*o* and *p*–*p* are two possible folding axes.

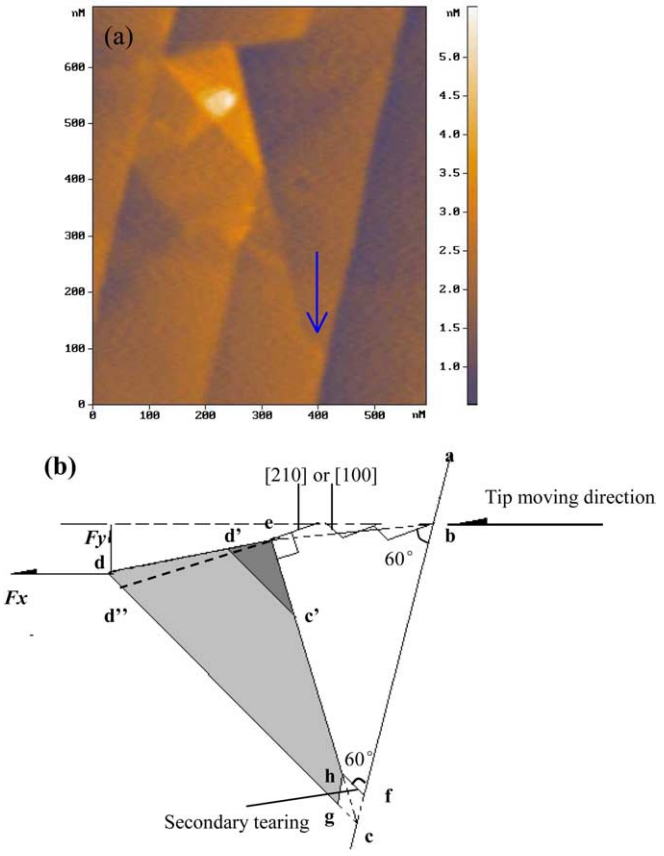

Fig. 4. Surface with one atomic layer (the larger folded triangle, $\triangle bec$) and three atomic layers (the smaller folded triangle, $\triangle d'ec'$) torn because the tip went through two steps on the fresh graphite surface. And a secondary breaking, pointed by the arrow in (a) and outlined by *fh* in (b) took place. Noticing that the angle, $\angle abe$, between the breaking and the step is about 110°, and the torn part $\triangle dec$ cannot fit the folded part $\triangle bec$ (the same as $\triangle d''ec$). Because of the difference in the moving direction of the tip and the breaking direction of the network, *be*, a force component F_y along *Y*-axis is produced. Due to this force, the breaking took place in a zigzag way, the mixture of [2 1 0] with [1 0 0] on the micro-scale.

Through a great deal of experiments, it was found that the folding axes are always along the symmetry axes of graphite, without any exceptions. But the breaking is not all the time along the symmetry directions of the network. One of these cases is shown in Fig. 4a. The breaking direction, *be*, is 110° to the step, *abc*, less than 120°, as outlined in Fig. 4b. Because of the difference between the tip moving direction and the breaking direction, a component force F_y was produced. The existence of the secondary breaking, pointed by the arrow in Fig. 4a and outlined by *fh* in Fig. 4b, can be a piece of evidence of the existence of the component force F_y. Due to the existence of F_y, the breaking direction, *be*, may be zigzag, the mixture of [2 1 0] with [1 0 0] on the micro-scale. The result is that the breaking direction is different from the symmetry directions of the graphite, even though it seems to be straight on the macro-scale.

Careful measurement reveals that the torn part, $\triangle dec$, cannot fit the folded part, $\triangle bec$, with the former larger than the latter, which is clearly illustrated in Fig. 4b. Such a phenomenon has been observed for many times in the experiments. It can be concluded that the torn part was stretched and could not resume its original shape after it was released from the tip. Due to the difference between the tip moving direction and the breaking direction, stretching of the torn part may cause deformation. If the deformation is small, the torn part will resume its original shape, $\triangle d''ec$, after it is released from the tip, as shown in Fig. 4b. This deformation is elastic. But if the deformation is severe, the Stone–Wales transformation might happen, in which the 5–7–7–5 pair (topological defect) [13–15] forms somewhere in the torn part. Consequently, the torn part is changed into $\triangle dec$ by this topological defect and cannot resume its original shape spontaneously. This deformation is plastic.

4. Conclusions

The breaking, folding and deformation of one or two sp^2-bonded graphene layers were realized by AFM. Observations confirm that preferential directions of breaking and folding exist when the hexagonal structure of graphite is torn. Due to the difference between the AFM tip moving direction and the breaking direction, however, deviation of the breaking direction and even plastic deformation of the torn part of the layer took place. The deformation occurs possibly because a Stone–Wales transformation happened somewhere in the hexagonal network of the torn region.

Acknowledgement

The authors acknowledge the financial support from NSFC (Grant No. 50325103).

References

[1] Coulson CA. Valence. Oxford: Oxford University Press; 1952.
[2] Demczyk BG, Wang YM, Cumings J, Hetman M, Hans W, Zettl A, et al. Direct mechanical measurement of the tensile strength and elastic modulus of multiwalled carbon nanotubes. Mater Sci Eng A 2002;334:173–8.
[3] Iijima S. Helical microtubules of graphitic carbon. Nature 1991;354:54–8.
[4] Salvetat-Delmotte J-P, Rubio A. Mechanical properties of carbon nanotubes: a fiber digest for beginners. Carbon 2002;40:1729–34.
[5] Ruoff RS, Qian D, Liu WK. Mechanical properties of carbon nanotubes: theoretical predictions and experimental measurements. C R Physique 2003;4:993–6.
[6] Yu MF, Lourie O, Dyer MJ, Moloni K, Kelly TF, Ruoff RS. Strength and breaking mechanism of multiwalled carbon nanotubes under tensile load. Science 2000;287:637–40.
[7] Wong EW, Sheehan PW, Lieber CM. Nanobeam mechanics: elasticity, strength and toughness of nanorods and nanotubes. Science 1997;277:1971–5.
[8] Salvetat J-P, Andrew G, Briggs D, Bonard JM, Bacsa R, Kulik AJ, et al. Elastic and shear moduli of single-walled carbon nanotube ropes. Phys Rev Lett 1999;82:944–6.
[9] Kelly BT. Physics of Graphite. London: Applied Science; 1981, pp.1–2.
[10] Hiura H, Ebbesen TW, Fujita J, Tanigaki K, Takada T. Role of sp^3 defect structures in graphite and carbon nanotubes. Nature 1994;367:148–51.
[11] Roy H-V, Kallinger C, Sattler K. Study of single and multiple foldings of graphitic sheets. Surf Sci 1998;407:1–6.
[12] Roy H-V, Kallinger C, Marsen B, Sattler K. Manipulation of graphitic sheets using a tunnelling microscope. J Appl Phys 2002;83:4695–9.
[13] Nardelli MB, Yakobson BI, Bernholc J. Mechanism of strain release in carbon nanotubes. Phys Rev Lett 1998;81:4656–9.
[14] Yakobson BI. Mechanical relaxation and intramolecular plasticity in carbon nanotubes. Appl Phys Lett 1998;72:918–20.
[15] Belytschko T, Xiao SP, Schatz GC, Ruoff RS. Atomistic simulation of nanotube fracture. Phys Rev B 2002;65:235430–7.
[16] Nardelli MB, Yakobson BI, Bernholc J. Mechanism of strain release in carbon nanotubes. Phys Rev B 1998;57:R4277–80.